

COMMENT

10.1002/2017JA023880

Key Points:

- The separation of the O- and X-mode effects by Wang et al. (2016) is incorrect
- The analysis of UHF radar observations by Wang et al. (2016) is failed and incorrect
- Wang results not in agreement with observational facts

Correspondence to:

N. F. Blagoveshchenskaya,
natally@ari.nw.ru

Citation:

Blagoveshchenskaya, N. F., Borisova, T. D., & Yeoman, T. K. (2017). Comment on "Parametric instability induced by X-mode wave heating at EISCAT" by Wang et al. (2016). *Journal of Geophysical Research: Space Physics*, 122. <https://doi.org/10.1002/2017JA023880>

Received 9 JAN 2017

Accepted 20 SEP 2017

Accepted article online 27 NOV 2017

Comment on "Parametric Instability Induced by X-Mode Wave Heating at EISCAT" by Wang et al. (2016)

N. F. Blagoveshchenskaya¹, T. D. Borisova¹, and T. K. Yeoman² 

¹Department of Geophysics, Arctic and Antarctic Research Institute, St. Petersburg, Russia, ²Department of Physics and Astronomy, University of Leicester, Leicester, UK

Abstract In their recent article Wang et al. (2016) analyzed observations from EISCAT (European Incoherent Scatter) Scientific Association Russian X-mode heating experiments and claimed to explain the potential mechanisms for the parametric decay instability (PDI) and oscillating two-stream instability (OTSI). Wang et al. (2016) claim that they cannot separate the HF-enhanced plasma and ion lines excited by O or X mode in the EISCAT UHF radar spectra. Because of this they distinguished the parametric instability excited by O-/X-mode heating waves according to their different excitation heights. Their reflection heights were determined from ionosonde records, which provide a rough measure of excitation altitudes and cannot be used for the separation of the O- and X-mode effects. The serious limitation in their analysis is the use of a 30 s integration time of the UHF radar data. There are also serious disagreements between their analysis and the real observational facts. The fact is that it is the radical difference in the behavior of the X- and O-mode plasma and ion line spectra derived with a 5 s resolution, which provides the correct separation of the X- and O-mode effects. It is not discussed and explained how the parallel component of the electric field under X-mode heating is generated. Apart from the leakage to the O mode, results by Wang et al. (2016) do not explain the potential mechanisms for PDI and OTSI and add nothing to understanding the physical factors accounting for the parametric instability generated by an X-mode HF pump wave.

Plain Language Summary In their recent article Wang et al. (2016) analyzed results from EISCAT (European Incoherent Scatter) Scientific Association active experiments and claimed to explain the potential mechanisms for processes occurring in the near-Earth space environment. There are serious disagreements between their analysis and the real observational facts. We reanalyzed the observations described by Wang et al. (2016) (WANG2016) and demonstrated that their results are flawed and incorrect. We then review WANG2016 step by step to disclose the flaws and failures of their analysis of observations.

1. Introduction

The growing body of X-mode experiments at the EISCAT (European Incoherent Scatter) Scientific Association HF heating facility with the use of various multi-instrument diagnostics showed that extraordinary (X-mode) powerful HF radio waves are capable of producing a strong modification of the high latitudinal ionospheric F region, including the generation of the artificial field-aligned irregularities (FAIs) (Blagoveshchenskaya, Borisova, Yeoman, Rietveld, 2011; Blagoveshchenskaya, Borisova, Yeoman, Rietveld, Ivanova, et al., 2011; Blagoveshchenskaya et al., 2013), optical emissions at red (630 nm) and green (557.7 nm) lines (Blagoveshchenskaya et al., 2014), and various spectral components in the narrowband stimulated electromagnetic emission spectra (Blagoveshchenskaya et al., 2015). Considerable study has been given to the HF-enhanced ion and plasma lines (HFILs and HFPLs) from the EISCAT UHF incoherent scatter radar spectra excited under X-mode heating, which are the signatures of the ion acoustic (IA) and Langmuir (L) electrostatic waves (Blagoveshchenskaya et al., 2014, 2015). The IA and L waves are attributed to the parametric decay (PDI) (Fejer, 1979; Hagfors et al., 1983; Perkins, Oberman, & Valco, 1974). The appearance of a nonshifted component in the ion line spectrum is indicative of the excitation of the modulation instability, also known as oscillating two-stream instability (OTSI) (DuBois, Rose, & Russell, 1993; Fejer, 1979). It was found that, generally, the X-mode HFILs and HFPLs demonstrate similar behavior and features in the overdense and underdense ionosphere (when the pump frequency is both below and above the critical frequency f_oF_2) (Blagoveshchenskaya et al., 2014, 2015). It is significant that the intense HFILs and HFPLs were excited when the X-mode pump wave was radiated toward the magnetic zenith while they were not excited for the vertical X-mode injections (Blagoveshchenskaya et al., 2015).

Some theoretical investigations related to the excitation of the parametric instabilities by the X-mode waves have been performed. Fejer and Leer (1972) suggested that the parametric electromagnetic instability could be excited when the HF pump wave has an extraordinary polarization. Here the exciting wave has an extraordinary polarization and the excited HF wave has the ordinary polarization. Both are electromagnetic waves in this case. Vas'kov and Ryabova (1998) proposed that extraordinary HF pump wave can generate the upper hybrid waves as well as enhancements of low-frequency plasma waves as a result of pump-induced scattering by ions. Fejer and Leer (1972) demonstrated that an X-mode pump wave is capable of exciting electrostatic waves in the Bernstein mode whose propagation vector is normal to the external magnetic field and whose frequency is that of the incident wave. Further, Sharma et al. (1994) proposed the parametric decay instability of X-mode pump waves into electrostatic electron Bernstein (EB) and ion Bernstein waves. Mishin, Hagfors, and Kofman (1997) and Kuo, Koretzky, and Lee (1998) have shown that Z mode (slow extraordinary wave) may decay into electron Bernstein (EB) and lower hybrid waves, the latter tending to collapse, with subsequent acceleration of electrons. The accelerated electrons enhance Langmuir waves, the source of the HFPL observed at EISCAT. Gelinis et al. (2003) reported on low-frequency density perturbations observed near the Z-mode reflection height during the rocket experiment at Arecibo.

In their recent article Wang et al. (2016), henceforth WANG2016, claimed to investigate the potential mechanisms and to understand the physical factors accounting for the parametric decay instability (PDI) and oscillating two-stream instability (OTSI) generated by an X-mode pump wave by analyzing the HF-enhanced ion and plasma lines (HFILs and HFPLs). They used the UHF radar data from the EISCAT Madrigal database collected from three Russian EISCAT HF heating experiments on 19 October 2012, 21 February 2013, and 22 October 2013. The first is observations published by Blagoveshchenskaya et al. (2014); the other two have no reference leaving a reader with the impression that these are Wang's et al. experimental results. HF heating experiments were planned and carried out by Dr. Blagoveshchenskaya and her team. To think up and to perform a successful experimental campaign requires significant efforts and expertise, and it is important to give proper credit to those who make such experiments a success. The campaign authorship details are shown in the Madrigal database and should be quoted when the data are used.

WANG2016 distinguished the O- and X-mode parametric instability in accordance with the different reflection altitudes of the O- and X-mode HF pump wave. Their reflection heights were determined from ionosonde observations (ionograms) between heater pulses. The threshold electric field for the parametric decay instability excited by an X-mode pump wave is also investigated and compared with the experimental observations.

In this comment we demonstrate that analysis and interpretation of our EISCAT heating experiments described by WANG2016 is flawed. We also show that the separation of O- and X mode effects used by WANG2016 is incorrect. The separation of the O- and X-mode effects plays a crucial role in the further analysis of the PDI and OTSI. The subsequent analysis by WANG2016 fails if such separation is incorrect. We present the separation procedure of the HF-induced ion and plasma lines excited by the X- and O-mode pump waves based on the specific features and distinctions between the UHF radar spectra. Then we briefly analyze the UHF radar observations in the course of O-/X-mode Russian EISCAT HF heating experiments described by WANG2016 with the use of the proposed UHF radar spectra separation. We then review WANG2016 step by step to disclose the flaws and failures of their analysis of observations, separation of the O- and X-mode effects, and analysis of the parametric decay instability excited by the X-mode pump wave.

2. The Separation of the X- and O-Mode Effects From EISCAT UHF Radar Spectra

Below we present experimental results showing the distinctive features and evolution of HF-enhanced ion and plasma lines (HFILs and HFPLs) induced by the extraordinary and ordinary polarized HF pump waves in the course of our experiment on 21 February 2013 (case 3 by WANG2016). An overview of phenomena from the EISCAT UHF radar observations in the course of an alternating O-/X-mode heating experiment on 21 February 2013 is shown in Figure 1. We would like to remind the reader that HF pumping was toward the magnetic zenith with the effective radiated power of about 530 MW at the heater frequency $f_H = 7.1$ MHz with alternating O-/X-mode polarization. In the course of the experiment the heater frequency was near or just above the critical frequency of the F_2 layer. Figure 1 shows the electron density and temperature (N_e and T_e), respectively; undecoded downshifted plasma line power; and raw ion line backscatter power

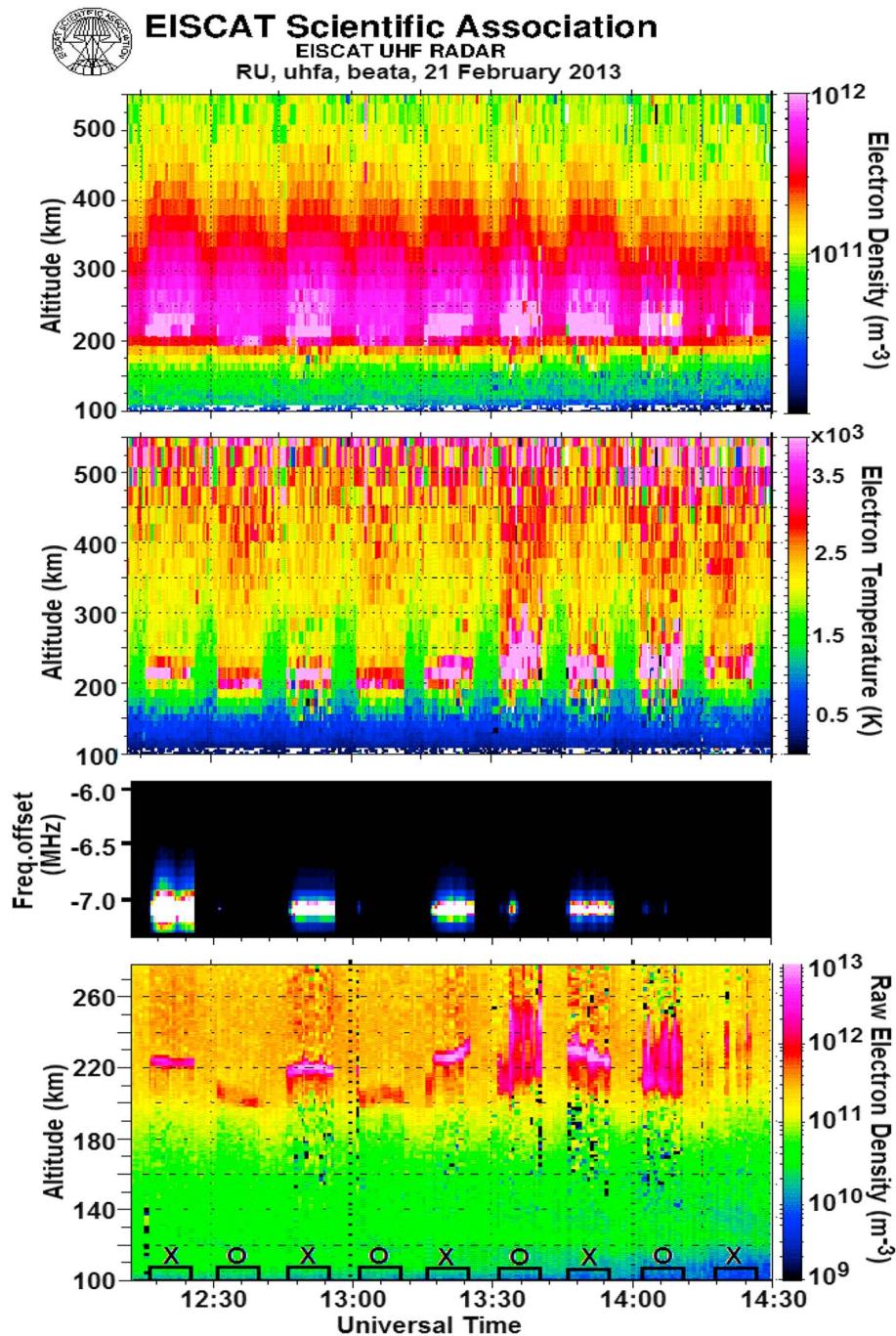


Figure 1. The behavior of the electron density (N_e) and temperature (T_e), undecoded downshifted plasma line power in the altitude range of 128–302 km, and the raw electron density (raw ion line backscatter power) from EISCAT UHF radar measurements with a 30 s integration time during alternating O-/X-mode pumping experiment on 21 February 2013 from 12:12 to 14:30 UT. HF pumping was produced toward the magnetic zenith with the effective radiated power of about 530 MW at the heater frequency $f_H = 7.1$ MHz by 10 min on, 5 min off pulses. The HF pump pulses and polarization of the heater wave are shown on the time axis.

(labeled as raw electron density) obtained from “raw” radar data with a 30 s integration time. As seen from Figure 1, the strong ion line backscatter power (Figure 1, bottom), which points to the excitation of HF-enhanced ion lines, was observed in all O- and X- mode pulses with the exception the last X-mode pulse from 14:16 to 14:26 UT, when $f_o f_2$ quickly dropped. From ionosonde records, which were used for the separation of the O- and X-mode effects in all analyzed cases, WANG2016 concluded that O-mode pump wave is not reflected from the ionosphere from 12:01 UT to 14:26 UT.

The excitation of X-mode HFILs was accompanied by strong HF-enhanced downshifted plasma lines observed throughout the whole heating pulse. The other situation was realized for O-mode cycles, in which the HFPLs excited only as response to the heater turned on in cycles from 12:31 to 12:41 and 13:01 to 13:11 UT. In the course of the O-mode cycles from 13:31 to 13:41 and 14:01 to 14:11 UT, HFPLs were observed sporadically. Here the HF pump wave starts partly to penetrate the ionosphere that leads to the strong and specific effects in the HFIL behavior and sporadic appearance of HFPLs. In fact, the experiment on 21 February 2013 is not typical at all, contrary to what WANG2016 concluded. Moreover, this experiment is not typical even in the stable ionosphere from 12:10 to 13:30 UT. As seen from Figure 1, the altitude of the X-mode HFILs was higher than the altitude of the O-mode HFILs throughout the time interval from 12:10 to 13:30 UT. Note that we did not analyze the first O-mode pulse from 12:01 to 12:11 UT owing to tuning up the HF heater at Tromsø.

Further we present the results of a detailed analysis and comparison between the plasma and ion line spectra derived from raw UHF radar data with a 5 s resolution, excited by O- and X-mode heating wave on 21 February 2013. We have chosen and compared two consecutive heater pulses at the heater frequency $f_H = 7.1$ MHz from 12:46 to 12:12.56 UT (X mode) and 13:01 to 13:11 UT (O mode) and at $f_H = 5.423$ MHz from 14:31 to 14:41 (O mode) and 14:46 to 14:56 UT (X mode). The main attention was paid to the growth time of HFPLs and HFILs after the heater turned on. Figure 2 shows the behavior of maximum power of HF-enhanced downshifted plasma lines and upshifted and downshifted ion lines (on a logarithmic scale) on 21 February 2013 at fixed altitudes during 2.5 min intervals starting 30 s before the heater turned on for O- and X-mode heating at $f_H = 7.1$ MHz (Figure 2a) and 5.423 MHz (Figure 2b). The power of the HFPLs and HFILs was found as the maximum in spectra derived every 5 s with 3 km altitude steps. During pump pulses the reflection altitude of the pump wave may be approximated by the altitude of the HF-enhanced ion line. The possible reflection heights derived from the electron density profiles from the EISCAT UHF radar 30 s before the pump onset are estimated at $f_H = 7.1$ MHz as about 232 and 220 km for the O- and X-mode waves, respectively, and at $f_H = 5.423$ MHz as 225 and 210 km for the O and X modes, respectively.

From Figure 2a (top row) it is clearly seen that the onset of the O-mode pump pulse at $f_H = 7.1$ MHz is accompanied by the abrupt increase of the intensity of the downshifted plasma line (HFPL) and upshifted and downshifted ion lines (HFIL_{UP} and HFIL_{DOWN}). They reached the maximum in the first 5 s data dump and then decayed in next few data dumps. It is the classic signature of the resonance parametric decay instability (PDI) (DuBois, Rose, & Russell, 1990; Fejer, 1979; Gurevich et al., 2004; Hagfors et al., 1983; Kuo, 2015; Perkins et al., 1974; Stubbe, Kohl, & Rietveld, 1992) when the O-mode HF pump wave decays into the Langmuir and ion-acoustic waves near the reflection height of the O-mode wave. PDI develops from the "cold" start, acts over few milliseconds of heating, and can be recognized in the EISCAT UHF radar spectra in the first few 5 s data dumps as HF-enhanced plasma and ion lines (initial overshoots) (Robinson, 1989). Thereafter, Langmuir and ion-acoustic waves are normally quenched by fully generated artificial small-scale field-aligned irregularities (FAIs) preventing further generation of the PDI (Stubbe, 1996). However, under high effective radiated power, the reappearance of the enhanced ion and plasma lines can occur after overshoots (Dhillon & Robinson, 2005; Mishin et al., 2016). Such a situation was observed during the O-mode pump pulse at $f_H = 7.1$ MHz when HF-enhanced upshifted and downshifted ion lines reappeared (see Figure 2a, top row).

Behavior of the enhanced plasma and ion line backscatters for X-mode pulse at $f_H = 7.1$ MHz differs radically from the O-mode one. As seen from Figure 2a (bottom row), HF-enhanced plasma and ion lines appeared not from the cold start, that is observed for O mode, but 15 s later. Thereafter, their power gradually increased and saturated within about 1 min.

The analogous behavior of the HF-enhanced ion and plasma line power was observed for O- and X-mode heating pulses at $f_H = 5.423$ MHz (see Figure 2b). The important point is that the heater frequency $f_H = 5.423$ MHz is close to the fourth electron gyroharmonic frequency, in the vicinity of which FAIs are suppressed. This results in the HF-enhanced plasma and ion lines being quenched by FAIs to a smaller degree (Stubbe, 1996). This is clearly seen from the behavior of HF-enhanced upshifted and downshifted ion lines (see Figure 2b, top row). As for X-mode pulse (Figure 2b, bottom row), the enhanced plasma and ion lines delayed within about 1 min after the heater turned on (T_0). Thereafter, they gradually increased and saturated within 2 min.

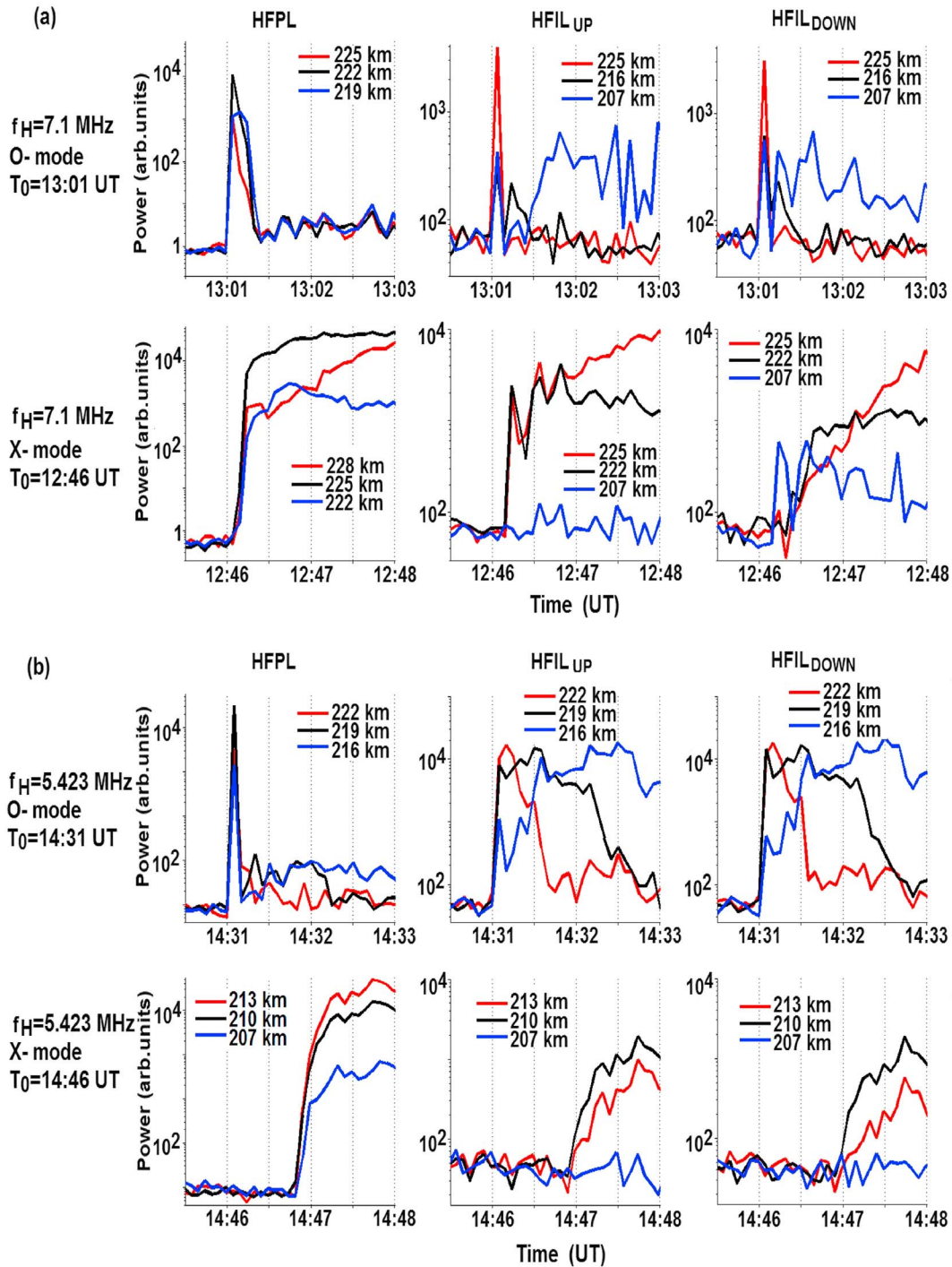


Figure 2. The maximum power of HF-enhanced downshifted plasma lines (HFPL), upshifted (HFIL_{UP}) and downshifted (HFIL_{DOWN}) ion lines at three fixed altitudes during 2.5 min intervals starting 30 s before the heater turned on for the O- and X-mode pulses derived from EISCAT UHF radar measurements on 21 February 2013. T_0 denotes the onset of the O-/X-mode transmission pulse. (a) The heater frequency $f_H = 7.1$ MHz. (b) The heater frequency $f_H = 5.423$ MHz. The power of the HFPLs and HFILs was derived as the maximum in spectra every 5 s with 3 km altitude steps.

Let us further consider the plasma and ion line spectra for O- and X-mode heating, which were derived from raw EISCAT UHF radar data at fixed altitudes with a 5 s resolution. Figures 3 and 4 show the downshifted plasma line spectra and ion line spectra at five altitudes for different times after HF pumping onset on 21 February 2013 at $f_H = 7.1$ MHz for the same O- and X-mode heating pulses as in Figure 2a. Figures 3a and 3b

illustrate the plasma line spectra for O- and X-mode pulses, respectively, and Figures 4a and 4b depict the ion line spectra for O- and X-mode pulses, respectively.

The intense plasma line spectrum appeared as immediate response to the O-mode pump onset and was seen in the first 5 s UHF radar data dump (13:01:05 UT). It possess the sharp peak shifted by the ion-acoustic frequency ("mother" Langmuir wave) and three intense downshifted cascade lines, so-called "daughter" Langmuir waves. In the next two 5 s dumps the O-mode plasma line spectra decayed and appeared at a lower altitude.

The X-mode plasma line spectrum appeared within 15 s after the HF pump onset at an altitude of 225 km, which is 3 km higher as compared to the initial appearance of O-mode enhanced plasma lines. Then the intensity of plasma line spectra gradually increased and saturated at 12:47:40 UT (after 100 s of HF pumping). At 12:48:50 UT the most intense plasma line spectrum displaced to 228 km. Weak cascade lines in the X-mode plasma line spectra can be also recognized.

The O-mode ion line spectra (Figure 4a), similar to the downshifted plasma line spectra, initially appeared at 13:01:05 UT in the first 5 s UHF radar data dump. They possess a strong peak at zero frequency and two intense shoulders, upshifted and downshifted from zero frequency by the ion-acoustic frequency. The presence of the peak at zero frequency in the UHF radar ion line spectrum indicates the excitation of the oscillating two-stream instability (OTSI) (DuBois et al., 1993; Fejer, 1979). Thereafter, the ion line backscatter displaced to lower altitudes from 225 km at 13:01:05 UT to 207 km at 13:01:50 UT, but its intensity was less as compared to the HF pump onset. Such descending ion line backscatter under O-mode heating was previously observed at the EISCAT/heating facility and High Frequency Active Auroral Research Program (HAARP) (Ashrafi et al., 2007; Dhillon & Robinson, 2005; Mishin et al., 2016; Pedersen et al., 2010). Notice that from 13:01:50 UT the ion line spectra appeared also at an altitude of 204 km (not shown in Figure 4a). From 13:02:10 UT their intensity was approximately the same as at 207 km. Ion line spectra were observed throughout the whole O-mode pump pulse.

The X-mode ion line backscatter developed at 12:46:15 UT within 15 s after the HF pump onset (see Figure 4b). The spectra exhibit only upshifted shoulders at altitudes of 219, 222, and 225 km (with the maximum at 222 km) and only downshifted shoulders at 207 km. Thereafter, their intensity gradually increased at altitudes of 222 and 225 km. From 12:46:35 UT the most intense ion line backscatter shifted 3 km higher to 225 km, which is the altitude of initial excitation of ion-acoustic waves under the O-mode heating (see Figure 4a). After 70 s pumping (12:47:10 UT) ion line spectra at 222 and 225 km possess upshifted and downshifted shoulders together with the weak zero component. The intensity of the ion line spectra, similar to the plasma line spectra, saturated 12:47:40 UT (after 100 s of HF pumping).

Figures 5 and 6 show the plasma and ion line spectra at five altitudes for different times after the pump onset on 21 February 2013 at $f_H = 5.423$ MHz for the same O- and X-mode pulses as in Figure 2b. Spectra are shown in the same manner as in Figures 3 and 4. As a whole, the distinctive features and development of the O- and X-mode plasma and ion line spectra are similar to those observed at $f_H = 7.1$ MHz. Namely, strongly enhanced ion and plasma line spectra under O-mode HF pumping appeared from the cold start immediately after the pump onset and were seen in the first 5 s radar data dump. Thereafter, the ion line backscatter layer descended to lower altitudes. The persistent O-mode ion line backscatter was observed both at $f_H = 7.1$ MHz and $f_H = 5.423$ MHz.

The X-mode ion and plasma lines delayed relative to the pump onset. Thereafter, their intensity gradually increased. However, there are some specific features at $f_H = 5.423$ MHz as compared to the 7.1 MHz case. The strength of the ion line spectra did not decay too much through the O-mode heating pulse. This is explained by the proximity of the pump frequency to the fourth electron gyroharmonic frequency, where FAIs are suppressed and ion lines are quenched to a smaller degree. As for the X-mode pulses, HF-enhanced ion and plasma lines developed after much longer delay time of about 60 s. The X-mode plasma and ion line spectra exhibit a very strong zero component, pointing to the OTSI excitation.

We have also considered the development of the plasma and ion line spectra derived from the EISCAT UHF raw data with a 5 s temporal resolution on 22 October 2013 (case 1 from WANG2016). As example, Figure 7 presents the downshifted plasma line spectra (Figure 7a) and ion line spectra (Figure 7b) at five altitudes for different times after the pump onset at $f_H = 7.1$ MHz for the X-mode pulse from 16:01 to 16:11 UT. As seen

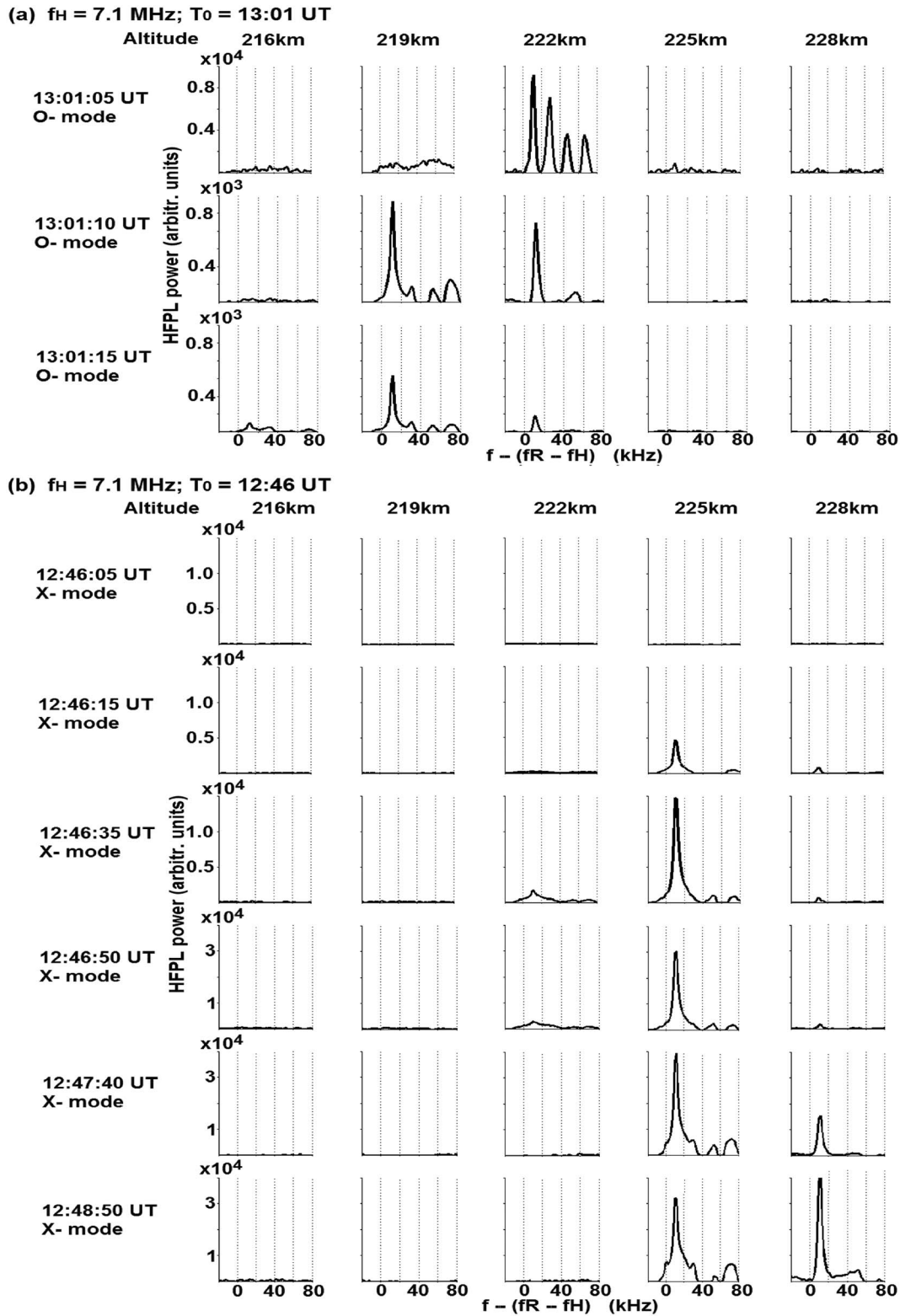


Figure 3. The downshifted plasma line spectra derived from the EISCAT UHF raw data with a 5 s resolution at five fixed altitudes for different times after the HF pump onset on 21 February 2013 at $f_H = 7.1$ MHz. T_0 denotes the onset of the O/X transmission pulse. (a) The O-mode transmission pulse. The scale of power was changed at 13:01:10 UT due to the strong attenuation of the plasma line spectra. (b) The X-mode pulse. The scale of power was changed at 12:46:50 UT due to the strong enhancement of the plasma line spectra.

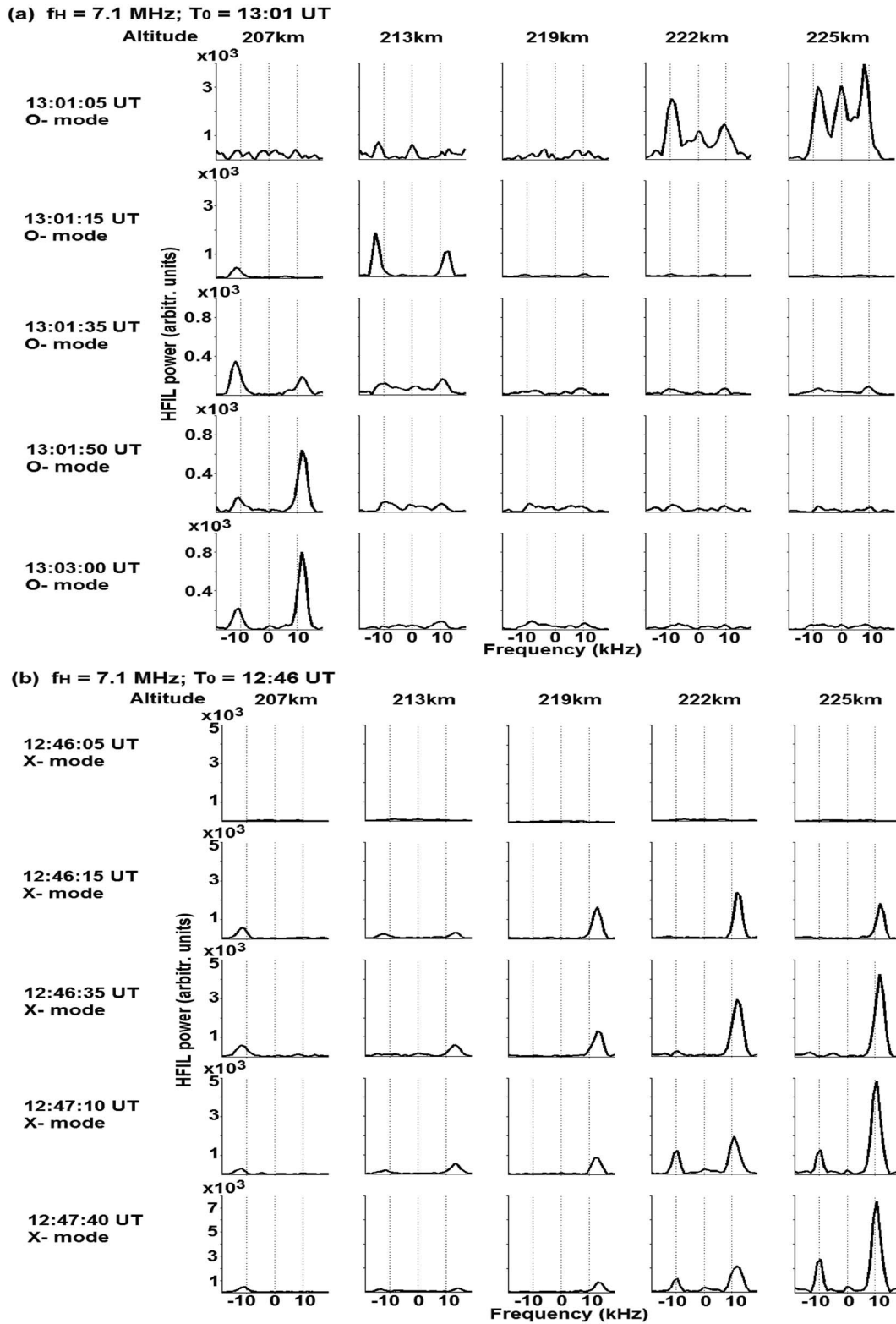


Figure 4. The ion line spectra derived from the EISCAT UHF raw data with a 5 s resolution at five fixed altitudes for different times after the HF pump onset on 21 February 2013 at $f_H = 7.1$ MHz. T_0 denotes the onset of the O/X transmission pulse. (a) The O-mode transmission pulse. The scale of power was changed at 13:01:35 UT due to the attenuation of the downshifted plasma line spectra. (b) The X-mode pulse. The scale of power was changed at 12:47:40 UT due to the enhancement of the downshifted plasma line spectra.

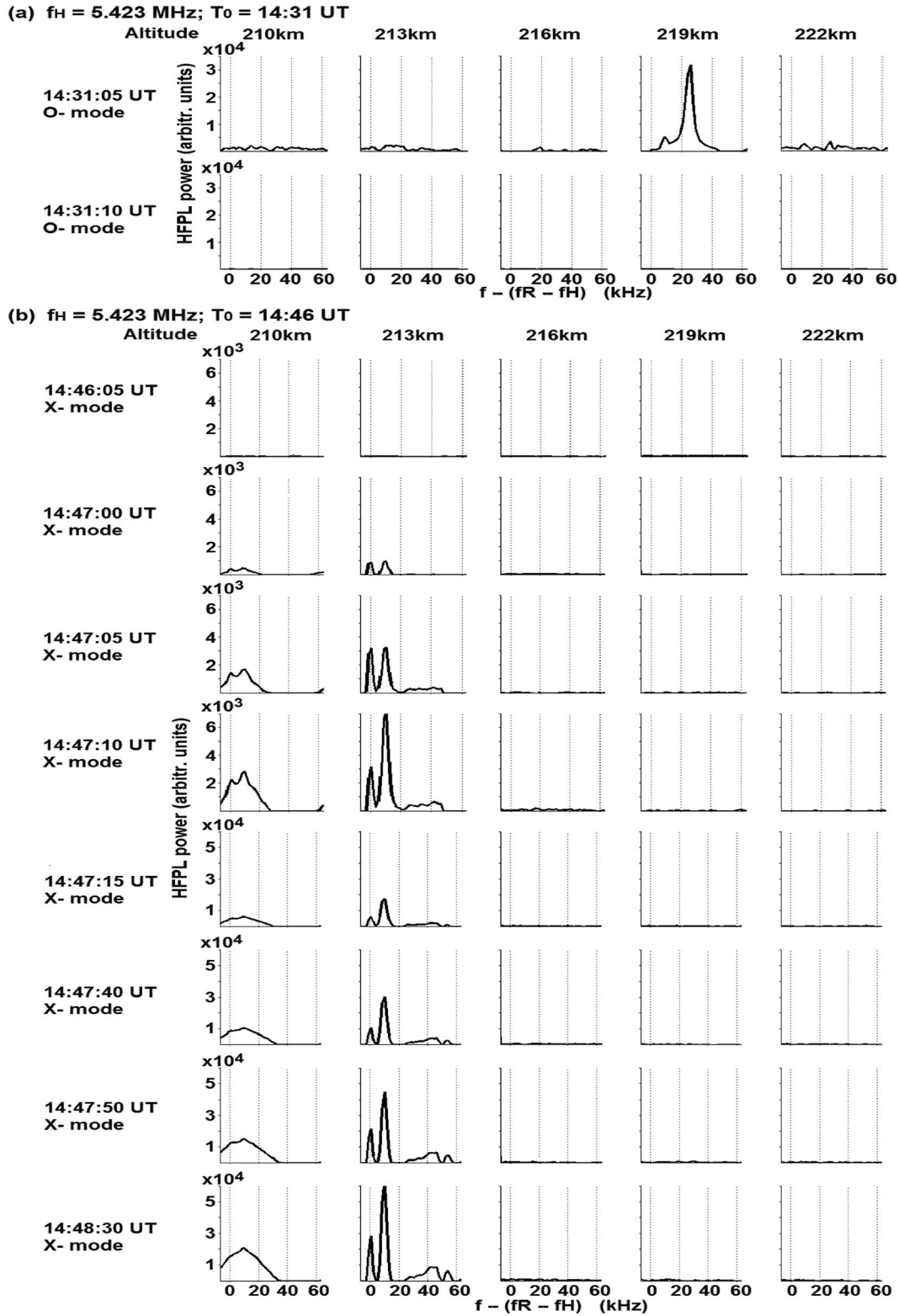


Figure 5. The same as in Figure 3 but at $f_H = 5.423$ MHz. T_0 denotes the onset of the O-/X-mode transmission pulse. (a) The O-mode transmission pulse. (b) The X-mode pulse. The scale of power was changed at 14:47:15 due the strong enhancements of the plasma line spectra.

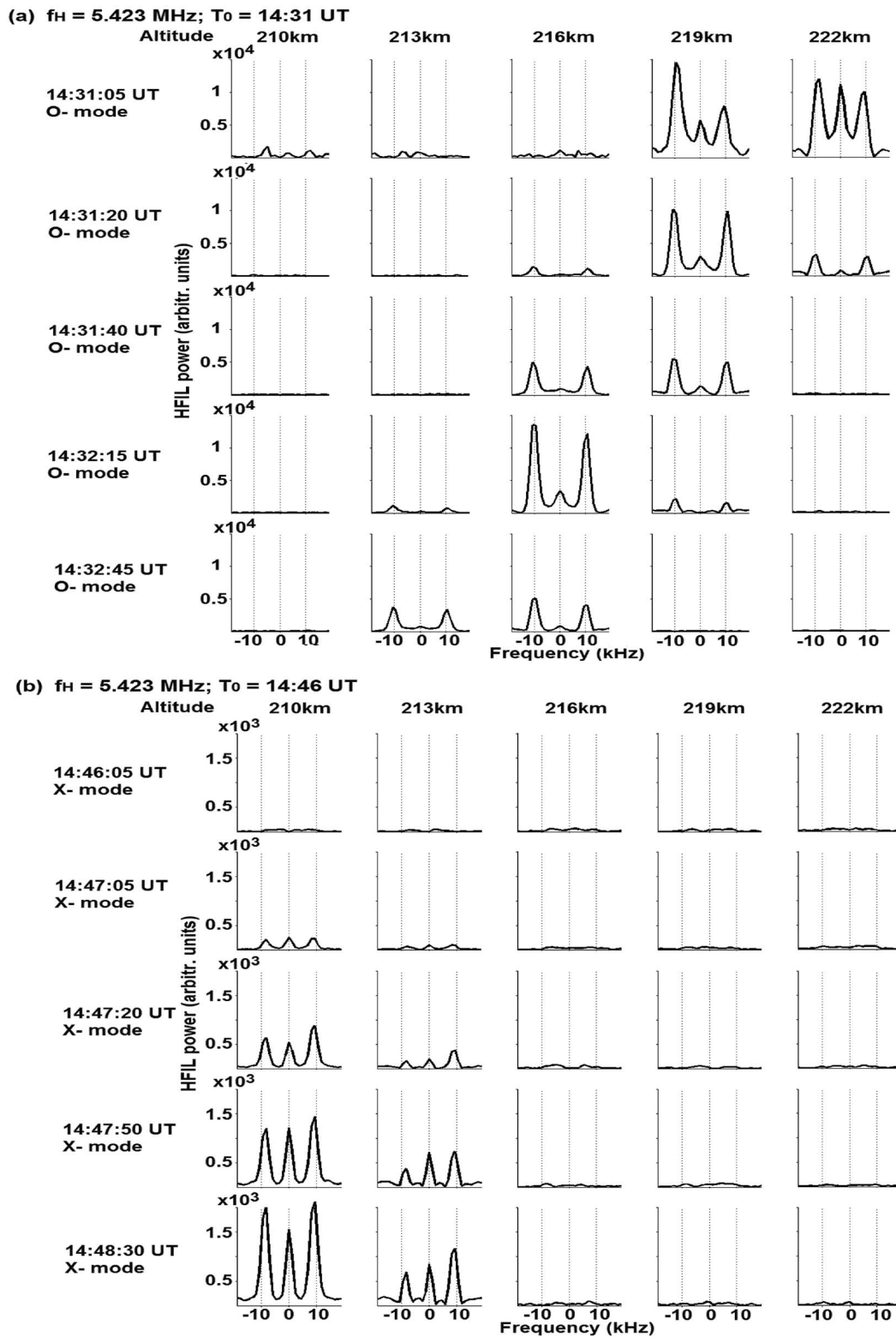


Figure 6. The same as in Figure 4 but at $f_H = 5.423$ MHz. T_0 denotes the onset of the O-/X-mode transmission pulse. (a) The O-mode transmission pulse. (b) The X-mode pulse.

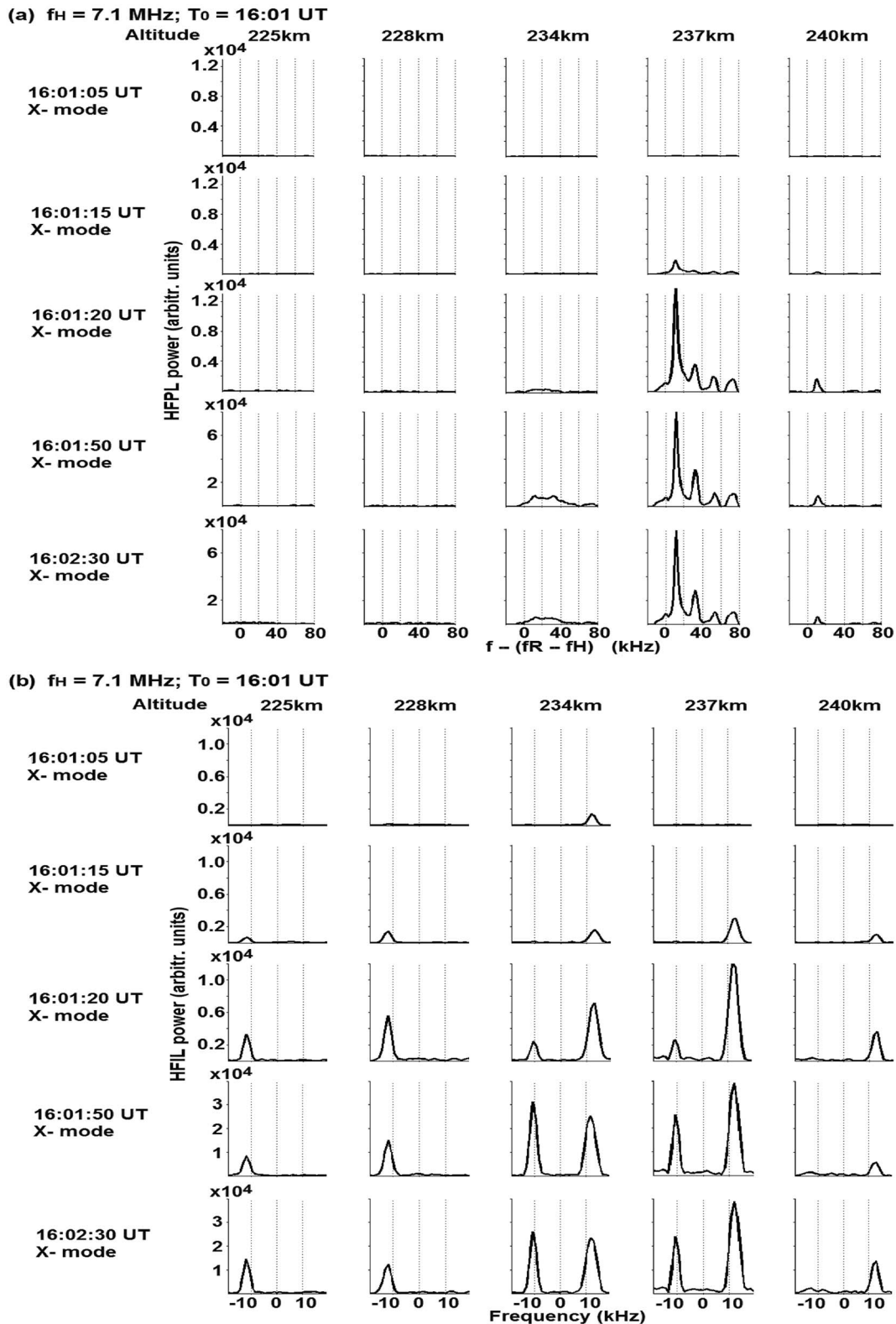


Figure 7. Plasma and ion line spectra derived from the EISCAT UHF raw data with a 5 s resolution on 22 October 2013 at five altitudes for different times after the onset of the transmission pulse at $f_H = 7.1$ MHz. T_0 denotes the onset of the X-mode transmission pulse. (a) The plasma line spectra. (b) The ion line spectra. The X-mode HF pump wave with the effective radiated power of about 550 MW was radiated toward the magnetic zenith from 16:01 to 16:11 UT. The scale of powers was changed at 16:01:50 UT due to the strong enhancements of the plasma and ion line spectra.

from Figure 7, the plasma and ion line spectra clearly revealed features typical for X-mode pumping but not for O-mode pumping. Their intensities gradually increased and saturated at 16:01:50 UT within 50 s after the heater turned on, while in the course of O-mode heating the strongly enhanced ion and plasma line spectra appeared from the cold start in the first 5 s radar data dump. The specific feature in the behavior of ion line spectra was the presence of two maxima at different altitudes in the downshifted ion line intensities (see Figure 7b). The first maximum is located at 228 km, and the second one is at 237 km. The same feature was often observed in a large body of our X-mode experiments carried out at pump frequencies both below and above the critical frequency of the F_2 layer, $f_H \leq f_oF_2$ and $f_H > f_oF_2$ (Blagoveshchenskaya et al., 2014, 2015).

To summarize, the comparison between the X- and O-mode plasma and ion line spectra derived with a 5 s resolution clearly exhibits the radical differences that allows us to distinguish correctly the HF-enhanced plasma and ion lines (HFPLs and HFILs) excited by the X- and O-mode HF pump waves.

3. Discussion of WANG2016 Flows and Summary

We turn now to a step-by-step analysis of the WANG2016 flows. Their analysis fails due to the following reasons.

1. WANG2016 stated that “the HFPLs and HFILs excited by O- and X-mode pump waves cannot be separated in EISCAT UHF radar spectra.”

We propose to distinguish the O- and X-mode effects according to the development after the heater turned on and specific features of the HF-enhanced plasma and ion line spectra. The radical difference between the X- and O-mode plasma and ion line spectra derived with a 5 s resolution was clearly demonstrated in section 2 and Figures 2–7. Namely, under O-mode HF pumping the abrupt enhancements in the ion and plasma line spectra appeared from the cold start just immediately after the heater turned on and were seen in the first 5 s radar data dump. Thereafter, Langmuir and ion-acoustic waves are normally quenched by fully generated artificial small-scale field-aligned irregularities (FAls) preventing further generation of the PDI (Stubbe, 1996). However, under high effective radiated power conditions, the reappearance of the enhanced ion and plasma lines could occur after overshoots. Such a situation was observed during the O-mode pump pulse at $f_H = 7.1$ MHz when HF-enhanced upshifted and downshifted ion lines reappeared (see Figure 2a, top row, and Figure 4a).

The X-mode ion and plasma lines delayed relative to the pump onset. Thereafter, their intensity gradually increased and saturated within about 1 min or even longer. Plasma and ion line backscatter, coexisting with the strong artificial field-aligned irregularities, were observed through the whole transmission pulse (Blagoveshchenskaya et al., 2014, 2015).

2. WANG2016 stated that “the leakage to O-mode wave at least 2% - 3% ERP under X-mode heating in the course of the experiment on October 22, 2013”.

In the course of the experiment on 22 October 2013 the effective radiated power of the X-mode wave varied between 540 and 548 MW with a peak gain at azimuth Az 180° and Zen 12° (transmission was produced into the magnetic zenith, MZ). The leakage to the O-mode was about 10 MW with a peak gain at Az 359° and Zen 27°. It means that the transmission of the O-mode wave occurred in the northward direction under low-elevation angles, but not into the MZ, confirming that the leakage effect did not exceed 1%.

3. WANG 2016 stated that “the HFILs and HFPLs excited by O- or X-mode cannot be separated in the spectrum due to the power leakage problem”.

The power leakage effect to the O-mode wave in the course of the X-mode HF heating can be easily recognized from the growth time and specific features of the plasma and ion line spectra. Even if the power leakage is enough to exceed the excitation threshold of the PDI, the abrupt enhancements in the ion and plasma line spectra would appear just immediately after the pump onset in first 5 s radar data dump. In next few 5 s radar data dumps they are quenched by fully generated FAls. If the leakage effect is negligibly small, we would expect the appearance of the X-mode plasma and ion line delayed relative to the onset of HF pumping. Thereafter, their power would gradually enhance, saturating within about 1 min.

4. WANG2016 stated that “the parametric instability excited by O/X-mode pump wave in the course of the X-mode heating can be distinguished according to the different excitation heights.”

WANG2016 separated the O- and X-mode effects according to the reflection height of O- and X-mode waves taken from ionograms recorded between heater pulses. In the course of the X-mode experiment on 22 October 2013 (case 1 by WANG 2016) downshifted HF-enhanced ion lines were excited at two different altitudes. They concluded that two downshifted HFILs at different heights were produced by the X- and O-mode pump waves. Because of that they attributed the downshifted ion line at the O-mode reflection height to the small leakage to the O-mode during X-mode heating. As shown in section 2, in this case, the O-mode typical features should be observed near the reflection altitude in the first 5 s radar data dump (see Figures 2a, 3a, and 4a). The simultaneous appearance of two downshifted ion lines at different altitudes is a typical feature in a large number of our EISCAT X-mode experiments carried out both at pump frequencies $f_H < f_oF_2$ and $f_H > f_oF_2$ (Blagoveshchenskaya et al., 2014, 2015). In the latter case even the small O-mode leakage is completely excluded.

However, the analysis of the 5 s UHF radar plasma and ion line spectra on 22 October 2013 clearly revealed features typical for X-mode pumping (see Figure 7 in section 2). It is important that the excitation of the PDI and/or OTSI requires a parallel electric field of the HF pump wave near the reflection altitude. However, the electric field of the X-mode wave is perpendicular to the magnetic field. We could suggest that some effective mechanism at the reflection height of the X-mode wave is acting, providing the conversion of the transverse electric field into the parallel one. For example, Fejer and Leer (1972) suggested that an exciting X-mode HF pump wave at the reflection height could be converted into the excited O-mode electromagnetic wave through the electromagnetic instability. Other conversion mechanisms could also act during the X-mode heating. More careful studies, both theoretical and experimental, are required in order to find out the mechanisms of the partial conversion of the transverse electric field of the X-mode pump wave into the parallel one. The excited wave with the parallel electric field could penetrate to the transformation point near the O- or Z-mode reflection altitude and produce PDI/OTSI.

5. The analysis of alternating O-/X-mode experiment on 19 October 2012 (case 2 from WANG2016) is not correct.

The Figure 2 by WANG2016 is not consistent with observational facts. Overview of the undecoded downshifted plasma line power and ion line backscatter power (raw electron density) obtained from the EISCAT UHF raw radar data with a 30 s integration time in the course of the alternating O-/X-mode heating experiment on 19 October 2012 from 17 to 19 UT clearly demonstrated the appearance of HF-enhanced ion and plasma lines for every O- and X-mode pulse except for the last O-mode heater pulse from 18:46 to 18:56 UT. It is important that in the course of every transmission pulse the UHF radar was scanned in the elevation angle between 76 and 80° with 1° steps every 2 min. However, the analysis by WANG2016 did not take into account this important feature of the experiment. The strongest HFPLs and HFILs were observed in the vicinity of the magnetic field-aligned direction at Tromsø (77–79°). At $f_H = 6.2$ MHz the enhanced backscatter was observed in every transmission pulse. To the end of the O-mode pump pulse from 17:31 to 17:41 UT the heater wave penetrated the ionosphere, but in the next X-mode pulse from 17:46 to 17:56 UT, when f_H exceeded the critical frequency f_oF_2 ($f_H > f_oF_2$), sufficiently strong enhanced plasma and ion lines were excited near magnetic zenith (77–79°). At $f_H = 5.423$ MHz relatively strong HFILs and HFPLs were excited during the X-mode pulse from 18:01 to 18:11 UT and much weaker signatures only near the magnetic zenith could be seen from 18:31 to 18:41 UT. The O-mode HF pump wave penetrated the ionosphere from 18:16 to 18:26 UT. What was revealed from Figure 2 by WANG2016? They found the only X-mode transmission pulse in which the HF-enhanced plasma and ion lines were observed. However, the HFILs were also observed in the preceding O-mode pulse that is not seen in Figure 2 by WANG 2016. The comparison between the O- and X-mode effects and the excitation of the PDI and OTSI near the reflection altitude of the X-mode HF pump wave for the same pump pulses has already been shown by Blagoveshchenskaya et al. (2014).

6. WANG2016 stated that “according to the nearby ionosonde records, the O-mode heating wave penetrates out the ionosphere from 12:01 UT to 14:26 UT, which is the under-dense heating” (case 3 by WANG2016).

In the course of the experiment on 21 February 2013 the HFPLs and HFILs at 7.1 MHz were produced by both the O- and X-mode HF pump wave, as shown in section 2 and Figure 1. Thus, the O-mode wave was certainly reflected from the ionosphere. This confirms that reflection altitudes of the O- and X-mode waves, obtained

from the ionosonde records between the transmission pulses, while it provides a rough measure of such altitudes, could be incorrect and could not be used for the separation of the O- and X-mode effects.

7. WANG2016 stated that “strong HF-induced plasma and ion lines at pump frequency of 7.1 MHz were observed near the reflection height of the X-mode wave” (case 3 by WANG2016).

It is not evident at what altitudes they were excited. In section 2 we presented results of a detailed analysis and comparison between the plasma and ion line spectra derived from raw UHF radar data with a 5 s resolution, excited by O- and X-mode heating wave at $f_H = 7.1$ MHz (see also Figures 2a, 3, and 4). As seen from Figure 3, the X-mode downshifted plasma line spectrum appeared within 15 s after the pump onset (T_0) at an altitude of 225 km, which is 3 km higher as compared to the initial appearance of the O-mode plasma line spectrum in the first 5 s radar data dump. The X-mode ion line spectrum, similar to the plasma line spectra, also appeared within 15 s after T_0 at the same altitudes as the O-mode ion line spectrum in the first 5 s radar data dump (see Figure 4). Therefore, it is not possible to separate the O- and X-mode effects according to their reflection heights from ionosonde records between heater pulses alone as was done by WANG2016. However, the evolution of the enhanced plasma and ion line spectra after T_0 and their spectral features provide sufficient evidence to clearly distinguish the O- and X-mode effects.

8. WANG2016 stated that “ascending and descending echoes of the HFPLs and the HFILs are observed at X-mode heating periods...” (case 3 by WANG2016).

Ascending and descending echoes of the HFPLs and the HFILs by WANG2016 observed at X-mode heating periods from 13:16 to 13:26 UT and 13:46 to 13:56 UT were caused by background ionospheric changes. From 13:16 to 13:26 UT the background ionosphere dropped and reflection altitudes increased. In the course of the pump pulse from 13:46 to 13:56 UT the background ionosphere enhanced and reflection altitudes decreased. This has nothing to do with descending structures observed at the EISCAT/heating and HAARP under O-mode pumping, which were reported and discussed by Dhillon and Robinson (2005), Ashrafi et al. (2007), Pedersen et al. (2010), and Mishin et al. (2016). However, such descending ion line backscatter was observed at O-mode pumping at 7.1 and 5.423 MHz on 21 February 2013 and could be clearly recognized from Figures 4 and 6 in section 2.

9. WANG2016 stated that “no obvious plasma lines are observed during the O-mode heating cycle” (case 3 by WANG2016).

Such statement is incorrect. The intense HF-enhanced plasma lines under O-mode heating at 7.1 and 5.423 MHz were observed in the first 5 s UHF radar dump as shown in section 2 (see Figures 2a and 2b, top rows, and Figures 3a and 5a).

10. WANG2016 stated that “the electron temperature increases in every cycle of heater switching on” (case 3 by WANG2016).

Intense HF-enhanced ion lines were excited throughout the experiment on 21 February 2016. This does not make it possible to perform the proper estimations of the electron temperature (T_e) at the resonance altitude due to a high residual to the fitting. Estimations of the T_e in the course of the alternating O-/X-mode EISCAT heating experiment, when HFILs were not excited, were performed by Blagoveshchenskaya et al. (2015). It was shown that under X-mode heating the T_e increases were weak (about 20% above the background values), when the heater frequency was below the critical frequency f_oF_2 , and increased up to 50%, when f_H exceeded f_oF_2 . At the same time the O-mode heating demonstrated very strong T_e increases up to 300%, when $f_H \leq f_oF_2$.

11. WANG 2016 stated that “Figure 3 demonstrates the behavior of HFPLs and HFILs in the course of alternating O/X-mode heating experiment on February 21, 2013” (case 3 by WANG2016).

The Figure 3 by WANG2016 is not consistent with observational facts (see comments above for case 3 by WANG2016).

12. WANG2016 stated that “Table 1 summarizes the parametrically excited plasma waves observed in the three cases.”

The presence of downshifted HFPLs, upshifted, downshifted, and zero-offset ion lines in the Table 1 is incorrect due to the incorrect separation of the O- and X-mode effects (see all comments above and section 2).

13. WANG2016 stated that “Table 2 presents the threshold of the parallel electric field for exciting the parametric instability at the reflection heights of the X-mode heating wave for the three cases.”

Equations (9) and (10) by WANG2016 are appropriate to the case of “classic” resonance parametric decay instability/oscillating two-stream instability excited from the cold start as an immediate response to the pump onset and are seen as overshoot in the first few radar data dumps. It is realized under O-mode HF pumping at heater frequencies $f_H \leq f_oF_2$. The same is true for Figure 4 by WANG 2016. It is important that the O-mode FAls at EISCAT were generated for effective radiated power ERP < 4 MW O-mode waves (Wright et al., 2006).

The radically different behavior of the persistent Langmuir and ion-acoustic waves are typical for the X-mode HF pumping. They are excited, both at $f_H \leq f_oF_2$ and $f_oF_2 < f_H \leq f_xF_2$, not from the cold start, their intensity gradually enhanced and saturated within about 1 min. This clearly demonstrates the other type of the parametric instability, which, most likely, could be of nonresonance type and requires higher electric field threshold. More careful studies, both theoretical and numerical, are needed in order to detail the processes and mechanisms of the partial conversion of the X mode into O and Z mode. How the parallel component of the electric field under X-mode heating is generated, however, is not discussed and explained. Unfortunately, apart from the leakage to the O mode, results by WANG2016 do not explain the potential mechanisms for PDI and OTSI and do not add any ideas to understanding the physical factors accounting for parametric instability generated by an X-mode HF pump wave.

14. WANG2016 concluded that “HFPLs and HFILs observed at the reflection height of the X-mode heating wave provide direct evidence that the PDI or OTSI was excited during the X-mode heating periods.”

This was shown in more detail by Blagoveshchenskaya et al. (2014, 2015).

In summary we conclude the following.

We have found that the evolution of the X- and O-mode plasma and ion line spectra after the heater turned on clearly exhibits the radical difference. Under O-mode pumping the abrupt enhancements in the ion and plasma line spectra were seen in the first 5 s radar data dump. The X-mode ion and plasma lines delayed relative to the onset of HF pumping. Thereafter, their intensity gradually increased and saturated within about 1 min or even longer. Thus, the parametric decay instability excited by O-/X-mode pump wave can be distinguished according to their different development after the pump onset.

We have shown that an analysis of our EISCAT observations by WANG2016 is flawed. The serious limitation in their analysis and interpretation of the PDI/OTSI is the use of a 30 s integration time of the UHF radar data, which practically annihilate the difference in the development of the X- and O-mode effects. Their conclusions based on the incorrect separation of the X- and O-mode effects are wrong.

HF heating experiments analyzed by WANG2016 were planned and carried out by Dr. Blagoveshchenskaya and her team during EISCAT Russian heating campaigns. To think up and to conduct a successful experimental campaign requires the significant efforts and expertise, and it is important to give proper credit to those who make such experiments a success. The campaign authorship details are shown in the Madrigal database and should be quoted when the data are used. Own results by WANG2016 involved the data processing and theoretical interpretation. The former was incorrect and the latter did not add anything new to understanding the physical factors accounting for parametric instability generated by an X-mode HF pump wave.

Acknowledgments

EISCAT is an international scientific association supported by research organizations in China (CRIRP), Finland (SA), Japan (NIPR and STEL), Norway (NFR), Sweden (VR), and the United Kingdom (NERC). N.B. and T.B. are supported by Arctic and Antarctic Research Institute. T.K.Y. is supported by Science and Technology Facilities Council grant ST/H002480/1. We are greatly thankful to both reviewers for useful comments. The data used in this comment are available through the EISCAT Madrigal database (<http://www.eiscat.se/madrigal/>).

References

- Ashrafi, M., Kosch, M. J., Kaila, K., & Isham, B. (2007). Spatiotemporal evolution of radio wave pump-induced ionospheric phenomena near the fourth electron gyroharmonic. *Journal of Geophysical Research*, 112, A05314. <https://doi.org/10.1029/2006JA011938>
- Blagoveshchenskaya, N. F., Borisova, T. D., Yeoman, T. K., & Rietveld, M. T. (2011). The effects of modification of a high-latitude ionosphere by high-power HF radio waves. Part 1. Results of multi-instrument ground-based observations. *Radiophysics and Quantum Electronics*, 53(9-10), 512–531. <https://doi.org/10.1007/s11141-011-9247-y>
- Blagoveshchenskaya, N. F., Borisova, T. D., Yeoman, T., Rietveld, M. T., Ivanova, I. M., & Baddeley, L. J. (2011). Artificial field-aligned irregularities in the high-latitude F region of the ionosphere induced by an X-mode HF heater wave. *Geophysical Research Letters*, 38, L08802. <https://doi.org/10.1029/2011GL046724>
- Blagoveshchenskaya, N. F., Borisova, T. D., Yeoman, T. K., Rietveld, M. T., Häggström, I., & Ivanova, I. M. (2013). Plasma modifications induced by an X-mode HF heater wave in the high latitude F region of the ionosphere. *Journal of Atmospheric and Solar - Terrestrial Physics*, 105-106, 231–244. <https://doi.org/10.1016/j.jastp.2012.10.001>

- Blagoveshchenskaya, N. F., Borisova, T. D., Kosch, M., Sergienko, T., Brändström, U., Yeoman, T. K., & Häggström, I. (2014). Optical and ionospheric phenomena at EISCAT under continuous X-mode HF pumping. *Journal of Geophysical Research: Space Physics*, 119, 10,483–10,498. <https://doi.org/10.1002/%202014JA020658>
- Blagoveshchenskaya, N. F., Borisova, T. D., Yeoman, T. K., Häggström, I., & Kalishin, A. S. (2015). Modification of the high latitude ionosphere F region by X-mode powerful HF radio waves: Experimental results from multi-instrument diagnostics. *Journal of Atmospheric and Solar - Terrestrial Physics*, 135, 50–63. <https://doi.org/10.1016/j.jastp.2015.10.009>
- Dhillon, R. S., & Robinson, T. R. (2005). Observations of time dependence and aspect sensitivity of regions of enhanced UHF backscatter associated with RF heating. *Annales de Geophysique*, 23(1), 75–85. <https://doi.org/10.5194/angeo-23-75-2005>
- DuBois, D. F., Rose, H. A., & Russell, D. (1990). Excitation of strong Langmuir turbulence in plasmas near critical density: Application to HF heating of the ionosphere. *Journal of Geophysical Research*, 95(A12), 21,221–21,272. <https://doi.org/10.1029/JA095iA12p21221>
- DuBois, D. F., Rose, A. H. A., & Russell, D. (1993). Space and time distribution of HF excited Langmuir turbulence in the ionosphere: Comparison of theory and experiment. *Journal of Geophysical Research*, 98(A10), 17,543–17,567. <https://doi.org/10.1029/93JA01469>
- Fejer, J. A. (1979). Ionospheric modification and parametric instabilities. *Reviews of Geophysics and Space Physics*, 17(1), 135–153. <https://doi.org/10.1029/RG017i001p00135>
- Fejer, J. A., & Leer, E. (1972). Excitation of parametric instabilities by radio waves in the ionosphere. *Radio Science*, 7(4), 481–491. <https://doi.org/10.1029/RS007i004p00481>
- Gelinas, L. J., Kelley, M. C., Sulzer, M. P., Mishin, E., & Starks, M. J. (2003). In situ observations during an HF heating experiment at Arecibo: Evidence for Z-mode and electron cyclotron harmonic effects. *Journal of Geophysical Research*, 108(A10), 1382. <https://doi.org/10.1029/2003JA009922>
- Gurevich, A. V., Carlson, H. C., Medvedev, Y. V., & Zybin, K. R. (2004). Langmuir turbulence in ionospheric plasma. *Plasma Physics Reports*, 30(12), 995–1005. <https://doi.org/10.1134/1.1839953>
- Hagfors, T., Kofman, W., Kopka, H., Stubbe, P., & Ijnen, T. (1983). Observations of enhanced plasma lines by EISCAT during heating experiments. *Radio Science*, 18(6), 861–866. <https://doi.org/10.1029/RS018i006p00861>
- Kuo, S. (2015). Ionospheric modifications in high frequency heating experiments. *Physics of Plasmas*, 22(1), 012901. <https://doi.org/10.1063/1.4905519>
- Kuo, S. P., Koretzky, E., & Lee, M. C. (1998). Parametric excitation of lower hybrid waves by Z-mode waves near electron cyclotron harmonics at Tromsø. *Journal of Geophysical Research*, 103(A10), 23,373–23,379. <https://doi.org/10.1029/98JA01741>
- Mishin, E., Hagfors, T., & Kofman, W. (1997). On origin of outshifted plasma lines during HF modification experiments. *Journal of Geophysical Research*, 102(A12), 27,265–27,269. <https://doi.org/10.1029/97JA02448>
- Mishin, E., Watkins, B., Lehtinen, N., Eliasson, B., Pedersen, T., & Grach, S. (2016). Artificial ionospheric layers driven by high-frequency radiowaves: An assessment. *Journal of Geophysical Research: Space Physics*, 121, 3497–3524. <https://doi.org/10.1002/2015JA021823>
- Pedersen, T., Gustavsson, B., Mishin, E., Kendall, E., Mills, T., Carlson, H. C., & Snyder, A. L. (2010). Creation of artificial ionospheric layers using high-power HF waves. *Geophysical Research Letters*, 37, L02106. <https://doi.org/10.1029/2009GL041895>
- Perkins, F. W., Oberman, C., & Valco, E. J. (1974). Parametric instabilities and ionospheric modification. *Journal of Geophysical Research*, 79(10), 1478–1496. <https://doi.org/10.1029/JA079i010p01478>
- Robinson, T. R. (1989). The heating of the high latitude ionosphere by high power radio waves. *Physics Reports*, 179(2-3), 79–209. [https://doi.org/10.1016/0370-1573\(89\)90005-7](https://doi.org/10.1016/0370-1573(89)90005-7)
- Sharma, R. P., Kumar, A., Kumar, R., & Tripathi, Y. K. (1994). Excitation of electron Bernstein and ion Bernstein waves by extraordinary electromagnetic pump: Kinetic theory. *Physics of Plasmas*, 1(3), 522–527. <https://doi.org/10.1063/1.870796>
- Stubbe, P. (1996). Review of ionospheric modification experiments at Tromsø. *Journal of Atmospheric and Terrestrial Physics*, 58(1-4), 349–368. [https://doi.org/10.1016/0021-9169\(95\)00041-0](https://doi.org/10.1016/0021-9169(95)00041-0)
- Stubbe, P., Kohl, H., & Rietveld, M. T. (1992). Langmuir turbulence and ionospheric modification. *Journal of Geophysical Research*, 97(A5), 6285–6297. <https://doi.org/10.1029/91JA03047>
- Vas'kov, V. V., & Ryabova, N. A. (1998). Parametric excitation of high frequency plasma oscillations in the ionosphere by a powerful extraordinary radio wave. *Advances in Space Research*, 21(5), 697–700. [https://doi.org/10.1016/S0273-1177\(97\)01006-5](https://doi.org/10.1016/S0273-1177(97)01006-5)
- Wang, X., Zhou, C., Liu, M., Honary, F., Ni, B., & Zhao, Z. (2016). Parametric instability induced by X-mode wave heating at EISCAT. *Journal of Geophysical Research: Space Physics*, 121(10), 10,536–10,548. <https://doi.org/10.1002/2016JA023070>
- Wright, D. M., Davies, J. A., Yeoman, T. K., Robinson, T. R., & Shergill, H. (2006). Saturation and hysteresis effects in ionospheric modification experiments observed by the CUTLASS and EISCAT radars. *Annales de Geophysique*, 24(2), 543–553. <https://doi.org/10.5194/angeo-24-543-2006>